frontiers | Frontiers in Sustainable Food Systems

TYPE Original Research
PUBLISHED 09 August 2024
DOI 10.3389/fsufs.2024.1430624

OPEN ACCESS

EDITED BY
Claudia-Maria Simonescu,
Politehnica University of Bucharest, Romania

REVIEWED BY
Dobrinas Simona,
Ovidius University, Romania
Petre Chipurici,
National University of Science and Technology POLITEHNICA Bucharest, Romania
Aurel Diacon,
Military Technical Academy, Romania

*CORRESPONDENCE
Fozia Batool
✉ fozia.batoo@uos.edu.pk
Hayssam M. Ali
✉ hayhassan@ksu.edu.sa

RECEIVED 10 May 2024
ACCEPTED 25 July 2024
PUBLISHED 09 August 2024

CITATION
Tahira M, Batool F, Noreen S, Mustaqeem M, Munawar KS, Kanwal S, Shahbaz K, Arshad A and Ali HM (2024) Unlocking the potential of de-oiled seeds of *Citrus sinensis* loaded with metal nanoparticles for Congo red degradation and removal: a green water treatment strategy with bibliometric analysis. *Front. Sustain. Food Syst.* 8:1430624. doi: 10.3389/fsufs.2024.1430624

Unlocking the potential of de-oiled seeds of *Citrus sinensis* loaded with metal nanoparticles for Congo red degradation and removal: a green water treatment strategy with bibliometric analysis

Misbah Tahira[1], Fozia Batool[1]*, Sobia Noreen[1], Muhammad Mustaqeem[1], Khurram Shahzad Munawar[1,2], Samia Kanwal[1], Komal Shahbaz[1], Anila Arshad[3] and Hayssam M. Ali[4]*

[1]Institute of Chemistry, University of Sargodha, Sargodha, Pakistan, [2]Department of Chemistry, University of Mianwali, Mianwali, Pakistan, [3]Key Laboratory of Modern Agricultural Equipment and Technology, Ministry of Education, School of Agricultural Engineering, Jiangsu University, Zhenjiang, China, [4]Department of Botany and Microbiology, College of Science, King Saud University, Riyadh, Saudi Arabia

This research reported the utilization of novel adsorbent from the de-oiled waste material of orange seeds for preparing simple charcoal (SC) and iron oxide/activated charcoal (Fe_2O_3/AC) nanocomposites. Batch adsorption experiments were carried out to evaluate the optimized conditions of the experiment. The results obtained indicated that the pseudo-second-order kinetic model best fitted the adsorption data ($R^2 > 0.99$) and that the Freundlich isotherm model best explained the adsorption of dye on Fe_2O_3/AC. The adsorption process was spontaneous and exothermic in the temperature range of 293–333°K, as explained by calculated thermodynamic parameters, e.g., ΔG°, ΔH°, and ΔS°. The Fourier transform infrared (FTIR) spectroscopy results publicized that carboxyl and amine functional groups are present on the surface of adsorbents, which are responsible for the attachment of dye. The scanning electron microscopy (SEM) results showed that Fe_2O_3/AC has a porous surface and textual structure, which can efficiently adsorb dye molecules. A zetasizer was utilized for determining the size of the composites, and the thermal stability was determined by performing a thermogravimetric analysis (TGA). The findings of the comparative experiment indicated that Fe_2O_3/AC are more promising than raw activated carbon for the adsorption of Congo red (CR). The impregnation of iron oxide nanocomposites on an adsorbent resulted in an increased surface area-to-volume ratio, magnetic properties, and excellent reusable capacity. Overall, it can be reported as an innovative procedure promoting the recycling of waste products, which aids in protecting environmental and human health and in the development of the economy.

KEYWORDS

***Citrus sinensis* activated carbon, iron oxide activated carbon nanocomposites, green synthesis, Congo red, water pollution**

1 Introduction

The influx of waste products in the environment is a worldwide problem that has been spotlighted by several environmentalist groups. Water bodies are adulterated with colored effluents, chemicals, and contaminants from a variety of industries, including textile, pharmaceutical, food, cosmetics, beverage, paint, and leather industries (Chavan, 2011). The wastewater discharged from textile industries contains organic, inorganic, and other colored materials. Organic compounds, such as formaldehyde-based dye fixing agents, hydrocarbon-based softeners, chlorinated stain removers, and non-biodegradable dyeing chemicals, are all cancer-causing. These toxic chemicals can enter the food chain and result in water turbidity, hence increasing the level of risk to aquatic life and also increasing the cost of water treatment required to make it suitable for drinking purposes. Thus, studies related to treating wastewater that contains dyestuff are essential to reduce environmental pollution caused by dyestuff (Sarala and Venkatesha, 2006; Chavan, 2011).

Among the techniques used in textile manufacturing, dyeing causes significant issues because the surplus water is colored, with a high organic content. A kilogram of cloth manufactured by the textile industry demands 125 to 150 L of water. Approximately 100 tons of the 1,000 metric tons of dyes used by the textile industry each year leach into freshwater (Parvin et al., 2019). These effluents are highly colored and covered in foam when they are released into surface waterways since dyes are often surface active. This foam formation results in the decline of oxygen diffusion through the water's surface, limiting spontaneous oxidation's ability to purify the water. Moreover, dyes may be poisonous to water plants and animals, as well as humans. The color reduction of textile water is the most difficult task (Lin and Lin, 1993). These dyes are resistant to microorganisms and do not undergo biodegradation by aerobic biological treatments. The utilization of water and chemicals in the textile industry and the emancipated effluents exploit the environmental quality in textile-producing zones (Smith, 1986; Smith, 1988).

For the physical treatment of wastewater that contains dyes, techniques involving adsorption, membrane filtration, ion exchange, and electrochemical approaches are available (Akbari et al., 2002; Raghu and Basha, 2007; Shi et al., 2007; Banerjee and Chattopadhyaya, 2017). Physiochemical techniques, which incorporate coagulation, flocculation, ultrafiltration, ozonation, chemical oxidation, and electrochemical adsorption, have been thoroughly explored for color removal practices (Arslan et al., 2000; Wang et al., 2003; Al-Bastaki, 2004; Shi et al., 2007). Some biological techniques, such as activated sludge and bacterial action, can also be utilized (Banat et al., 1996; Martin et al., 2005). Adsorption, one of the cost-effective and efficient methods, is an emerging technique that is frequently used in dye adsorption from aqueous media (Sarioglu and Atay, 2006). Although activated carbon is the typically employed adsorbent for the treatment of wastewater (either in powdered or granular form), other adsorbents, including bentonite, barbecue charcoal, vermiculite, sawdust, dried crushed maize stalks, sand peat moss, and dried ground rice hulls, have also been scrutinized for color removal. Barbecue charcoal was discovered to be the most effective absorbent, with a 67% efficacy in color removal (Meyer et al., 1992). An activated carbon or activated sludge system is the most commonly employed adsorbent for this purpose as it has a large capacity for color adsorption, even though its application is restricted due to its high cost (Annadurai et al., 2002). Therefore, inexpensive substances such as natural clay, bagasse pith, maize cob, rice husk, garlic stalks, wood, waste orange peel, and banana pith are a few materials that have been explored as adsorbents for dyes (Astrazon Blue, Maxilon Red, and Telon Blue) in aqueous solutions (Nassar and El-Geundi, 1991).

Among many coloring agents, Congo red (CR) is a well-known synthetic dye that has several important uses. Congo red, an azo dye, is banned due to its cancerous effect on human health. They get into the bodies of aquatic animals and are converted into mutagenic materials, which eventually causes DNA mutations. Synthetic dyes, as they are non-biocompatible and non-biodegradable, hurt the aquatic ecology as they are converted into carcinogenic materials and pose a serious threat to life in water bodies and also to humans who feed on aquatic life (Kant, 2012). Due to their intricate chemical makeup, they are resistant to being broken down by chemical, physical, and biological treatments (Sahoo et al., 2022). Even at a concentration of 1 ppm, the presence of a dye in a body of water is exceedingly visible and alters the photosynthetic process of aquatic plants since it forbids sunlight from penetrating the water (Adegoke and Bello, 2015). According to previous reports, dyes are deleterious to humans and animals even when present in a concentration of 1 ppb (Rushing and Bowman, 1980). Consequently, the elimination of these colored effluents from the aqueous media is very necessary.

According to previous reports, nanohybrid composites based on iron oxide and ferrite (as inorganic components) have been extensively researched and successfully tested for the removal of dyes from aqueous solutions (Pour and Ghaemy, 2015; Song et al., 2016). Among the diverse nanomaterials used as adsorbents, hybrid magnetic nanocomposites (HMNCs) have captivated a lot of attention due to their unusual surface, magnetic, chemical, physiochemical, and mechanical stabilities (Lompe et al., 2017, 2018; Gong et al., 2023). Biochar and/or activated carbon (as an organic content) based HMNCs were found to be the best choice in terms of their utility; however, they necessitate high temperature and energy-consuming machinery, such as furnaces (Choudhry et al., 2021). Several alternatives to biochar and/or activated carbon-based HMNCs are being explored to synthesize environmentally friendly nanocomposites using iron oxide and/or ferrite (Sahraei et al., 2017). Recently, the development of nanocomposites based on natural plant resources, such as leaves, seeds, sprouts, gum, and mucilage, without converting them into biochar or activated carbon is getting the attention of researchers (Cai et al., 2010; Yuvaraja et al., 2020; Choudhry et al., 2021). According to previous studies, plant materials have cellulose surfaces, with a lot of functional groups that could interact with metal ions while synthesizing composites. In addition, plant compounds known as phytochemicals aid in stabilizing and capping the created substance. The final nanocomposites have small, highly functional sites and low production coefficients (Choudhry et al., 2021). These have a variety of uses, including antibacterial ones, photocatalysis, and, most precisely, adsorption (Rathi et al., 2020).

Citrus fruit production in Pakistan is growing at a very good pace, constituting approximately 30% of the total fruit production in the country. The waste products such as peel, seeds, and pomace, are disposed of. Several researchers have experimented with the utilization of these waste products as a green and cost-effective alternative to other synthetic adsorbents (Su et al., 2022; Khanpit et al., 2023). Iron oxide nanocomposites have gained eminent attraction in solving environment-related issues because these have strong

superparamagnetic and magnetic susceptibility, and hence, can be efficiently utilized in the synthesis of magnetic nanoadsorbents. Impregnating iron oxide nanocomposites on adsorbents results in an increased surface area-to-volume ratio, cost-effectiveness, attractive functional groups, excellent biocompatibility, better magnetic properties, convenient separation by applying a magnetic field, and efficient reusability. In addition, these nanocomposites can coordinate with other elements as they can exist in several oxidation states. Iron oxide nanoadsorbents have been found promising in removing different contaminants, such as chromium (Ilankoon, 2014), atrazine (Castro et al., 2009), lead (Yao et al., 2016), and methylene blue dye (Tan et al., 2012) from aqueous solutions. All these properties are in favor of experimenting with agriculture waste (orange seeds) impregnated with iron oxide nanocomposites for the purification of water from harmful dyes. The results of the application of this adsorbent, therefore, can be favorable for researchers.

Huge amounts of seeds are produced by juice factories. These seeds are de-oiled to produce orange oil, and the remaining material is thrown away as waste material. An effective method introduced in this regard, which has not been experimented with yet, is the usage of de-oiled seed waste for the synthesis of activated carbon and then the application of Fe_2O_3 nanoparticles on them. There was no available research based on the mitigation of Congo red dye using *Citrus sinensis* simple charcoal (SC) and Fe_2O_3/AC. Accordingly, the main objective of this study was to test the adsorption efficiency of AC and to improve the adsorption efficiency, surface-to-volume ratio, and easy separation of adsorbents from an aqueous solution. Fe_2O_3/AC was synthesized by the impregnation of iron oxide on SC. Morphological and structural confirmation and characterization of the synthesized adsorbents were explored. Kinetics isotherms and thermodynamics were also investigated. The results revealed this innovative combination (Fe_2O_3/AC) as a low-cost and green alternative to Congo red dye, which is harmful to humans and aqueous animals.

2 Materials and methods

The chemicals employed for this research were of an analytical grade to ensure the precision and accuracy of the research findings. All experimental solutions were prepared using distilled water. Fresh orange seeds were separated from the sweet oranges that were purchased from the local market of Sargodha, and cost-effective seeds were collected from household waste, agriculture farmhouse waste, mills waste, etc. Potassium hydroxide (KOH) (98–100%), ferric nitrate ($Fe(NO_3)_3.9H_2O$) (99%), and Congo red dye (Formula: $C_{32}H_{22}N_6O_6S_2{\cdot}2Na$; molecular weight: 696.66 g/mol and 99% purity) were purchased from Sigma-Aldrich and were utilized directly. Distilled water of an analytical grade from the Khushab Water Plant, the University of Sargodha, Sargodha, Pakistan, was used.

2.1 Synthesis of adsorbent

Orange by-products are available in huge amounts, and due to the huge quantity and perishable nature, they are leading to an environmental burden. These waste products, such as peel, seeds, and pomace, can provide environmental benefits if properly reused. Orange peel has already been proven to be a good adsorbent; hence, orange seeds were utilized for the present study. *C. sinensis* seeds were cleaned by washing with distilled water several times, sun-dried, and ground. By manually grinding, these seeds were reduced in size. Oil was extracted from the seeds using the Soxhlet apparatus by employing n-hexane as a solvent. The defatted seeds were washed thoroughly with water, milled, and sieved through a 60-mesh sieve.

To synthesize activated carbon, the ground *C. sinensis* seeds were further converted into activated carbon through the process of pyrolysis in a furnace under an inert atmosphere of 450°C for 1.5 h. Pyrolysis was performed under a limited supply of oxygen in a muffle furnace at a heating rate of 10°C/mint. The muffle furnace reduced the risk of contamination during the pyrolysis process, and the slow heating rate resulted in complete pyrolysis. Cellulose, hemicellulose, and lignin are important components of plant waste; hence, the pyrolysis resulted in materials with a high carbon content. It was converted into a black-colored mass, a harmless and easy-to-use adsorbent material. Charcoal has a higher amount of carbon ratio and a lower amount of hydrogen and oxygen. It has a high surface area with plenty of pores, which allow it to trap chemicals. Its efficiency was further enhanced by the loading of Fe_2O_3 nanoparticles.

The charcoal was suspended in 100 mL of an aqueous solution containing $Fe(NO_3)_3.9H_20$ (5.28 g) at 74.85°C. After continuous heating, the 1 M KOH solution heated at 69.85°C was added dropwise to precipitate the iron oxide. The resulting solution obtained was filtered, and the filtrate was dried at 60°C for 5 h in an oven. It was stored for further experiments (Figure 1).

2.2 Characterization of adsorbent

One essential factor for determining the results of one's work is the characterization of the adsorbent. The selected material was used to study the adsorption of Congo red dye from an aqueous solution. Characterization was necessary for determining the adsorption capacity and functional group analysis of the adsorbent. It also provided us details about the hydrogen, oxygen, and carbon ratio of the adsorbent, required to know the adsorption capacity. For functional group determination, Fourier transform infrared (FTIR) spectroscopy was employed using the Instrument Model Shimadzu AIM-8800. The adsorbent was studied by employing the diffused reflectance infrared Fourier transform (DRIFT) method, in which the sample was mixed with KBr and took its spectra. Surface morphology was analyzed using the scanning electron microscopy (SEM) instrument, FEI Nova, Nano-SEM 450, Lausanne, Switzerland. BET analysis was performed using Quantachrome Instruments, Model No. Autosorb IQ-C-MP-AG (2 Stat.) Viton ID 195400, Boynton Beach, FL, United States. For the BET analysis, the adsorption of gases, generally nitrogen, krypton, or argon, was performed. For the present study, the adsorption of nitrogen was performed to calculate the surface area. The size of the composites was determined using zeta potential and zetasizer (Model No: Joel JSM-IT100, Peabody, MA, United States). Thermogravimetric analysis was performed using an SDT650 thermal analyzer with a serial number (0650–0681) and IP (192.168.1.2) in a nitrogen atmosphere at a heating rate of 10°C/min. A sample of 17.5 mg was taken in an alumina sample holder and heated from room temperature to 800°C to study the thermogravimetric–differential thermal analysis (TG–DTA).

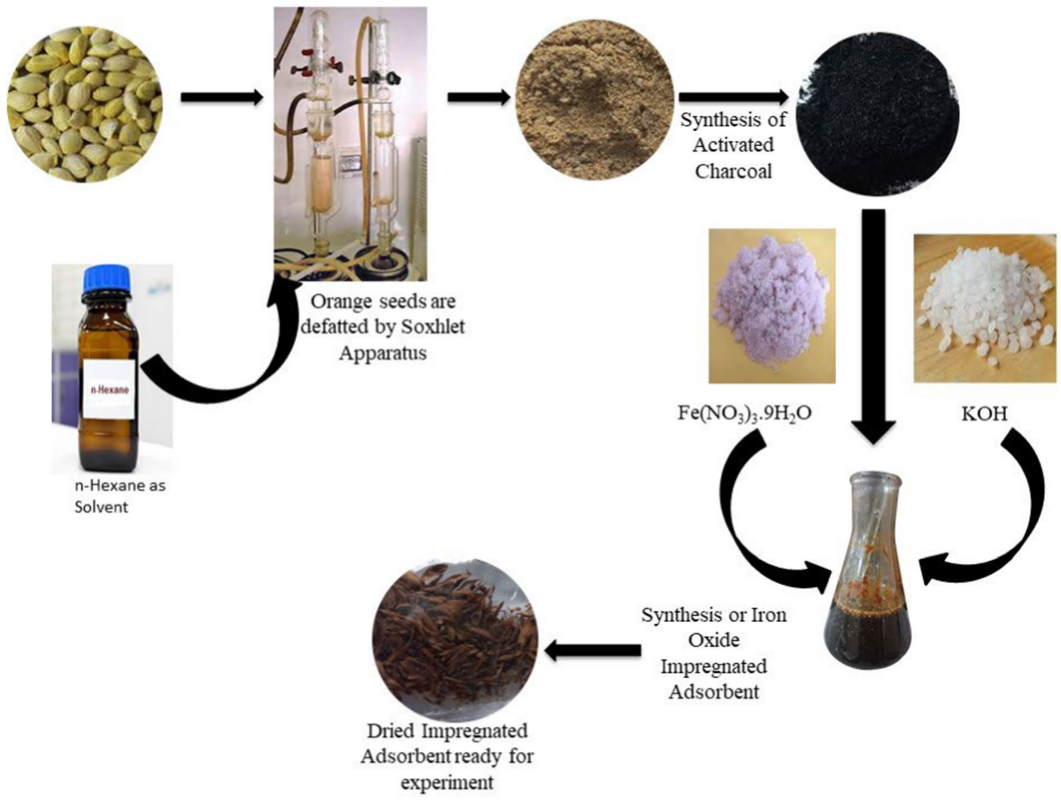

FIGURE 1
Scheme of synthesis of Fe_2O_3/AC for adsorption.

2.3 Batch experiment and parameters optimization

For the assessment of the adsorption capacity of SC and Fe_2O_3/AC, the procedure was as follows: the known 1 g adsorbent in 100 mL of the known concentration of Congo red was shaken with an orbital shaker at an agitating speed of 200 rpm for 3 h and then at an agitating speed of 320 rpm at room temperature. The solution was filtered, and the absorbance was measured at 498 nm using a UV–Visible spectrometer. The q_e and percentage removal were then calculated using equations, where C_i (mg/L) was the initial concentration, C_e (mg/L) was the equilibrium concentration, V (L) was the volume of solution, and m (g) was the mass of adsorbent used.

$$q_e = \frac{(C_i - C_e)}{m} \times V$$

$$\%R = \frac{(C_i - C_e)}{C_i} \times 100$$

The effect of different parameters, such as the initial concentration of the dye (20–100 ppm), adsorbent dosage (0.5–1.25 g), pH value (3–12), temperature (20–60°C), and contact time (30–120 min), were investigated. Parameter optimization was performed by varying the parameters.

The initial concentration of a dye is the most important factor of the adsorption phenomenon because by increasing the number of dye molecules, the adsorption potential of an adsorbent also increases up to a certain level of the dye concentration. After this concentration, the adsorption efficiency remains the same because of the occupation of all the active sites of the adsorbent. The contact time is the duration of interaction between the adsorbent and adsorbate, and it is investigated to confirm that the adsorption process has reached equilibrium. Increasing the dosage of the adsorbent increases the availability of adsorption sites for binding with the adsorbate (dye), thereby increasing the percentage removal. However, upon exceeding a certain level, the adsorption efficiency does not increase because of the overlapping of the adsorption sites (Tiadi et al., 2017). The pH value of the solution controls the electrostatic interaction between the adsorbent's surface and the adsorbate's functional groups (Razi et al., 2017).

2.4 Adsorption isotherm and kinetics

An adsorption isotherm must be created to study the adsorption process and the equilibrium relationship between a sorbent and sorbate. For this purpose, Freundlich, Langmuir, Dubinin–Radushkevich (D–R), and Temkin adsorption isotherms were applied to the experimental data. Similarly, pseudo-first-order and pseudo-second-order kinetic studies were also performed.

3 Results and discussion

The current research was performed with a special focus on green chemistry, and for this purpose, environment-friendly, non-toxic, and cost-effective de-oiled orange seeds were used for the preparation of SC and Fe_2O_3/AC. Impregnation of these iron nanocomposites will increase the adsorptive capacity of adsorbents in removing dyes for the purification of industrial wastewater.

3.1 Surface morphology study

Evaluation of the textual structure and morphology of the adsorbent surface, both before and after modification, was accomplished by performing scanning electron microscopy examinations. Micrographs were taken at different resolutions and magnifications. SEM images of all the treated biosorbents demonstrated that a simple biosorbent was a more compact fibrous material with fewer macropores (pores with a diameter > 50 nm). When compared to unmodified biosorbents, activated biosorbents exhibited more cavities in the fibrous components. These cavities served as an active site for the adsorption of dye molecules. A large number of entrapped iron oxide composites were also observed. The SEM findings were in line with the provided data (Figure 2).

As given in Figure 3, FTIR spectroscopy investigations were conducted to determine the functional group and chemical structure contained in the biomaterial and to assess how different dye molecules adhere to the composites' surface. The biosorbents' infrared spectra were captured in the 4,000–500 cm^{-1} wavelength region. The figure represents the FTIR spectra both before and after the adsorption of the dye. For simple and modified adsorbents, a band at 3407 cm^{-1} and 3,424 cm^{-1}, respectively, corresponded to O-H bond stretching. The width of the-OH group band in this area showed the presence of hydrogen bonds in these compounds. The additional peak of the N-H functional group was also present in the FTIR spectra of the modified adsorbent in the region of the O-H bond stretching. It was also determined that the CH_2 stretching band at 2932 cm^{-1} and 2,964 cm^{-1} was caused by the asymmetric stretching of CH_2 groups. The carbonyl groups of carboxylic acids were assigned to bands at 1751 cm^{-1} and 1701 cm^{-1} for simple and modified adsorbents, respectively (Alencar et al., 2012). The peak at 1518 and 1,552 cm^{-1} indicated the presence of Amide II. The peaks at 2268 cm^{-1} and 2038 cm^{-1} indicated the presence of an alkyne functional group. The peaks in the regions 1,002 and 1,026 cm^{-1} were associated with adsorption by C-O groups on the adsorbent surface. The presence of oxygen-containing functional groups resulted in additional active sites in the adsorption process. A peak observed at 1438 cm^{-1} and 1,446 cm^{-1} was C-H bending, which indicated the presence of alkane functional groups. These bands were enough to confirm the presence of methyl, hydroxyl, and carbonyl groups and aromatic structures on the adsorbent surface, which might have been responsible for the adsorption mechanism of Congo red onto the adsorbent (Adebisi et al., 2017; Niazi et al., 2018). The nanoparticles-impregnated adsorbent showed peaks for the presence of the Fe-O compound in the range of a 588 cm^{-1} wavenumber range. The origin of the stretching peaks of Fe-O can be explained as the use of Fe $(NO_3)_3.9H_2O$ for the preparation of activated charcoal nanocomposites. These results were also supported by kinetic and adsorption isotherms.

After the dye was attached to the composites, a decrease in the intensity of the adsorption peak was observed, or the peaks disappeared and new peaks were formed, which was due to the adsorption of the Congo red dye onto the adsorbent surface (Laskar and Kumar, 2017).

Zetasizer and zeta potential of the activated charcoal nanocomposites (before adsorption) were performed. Dispersant RI and viscosity were found to be 1.330 and 0.8872, respectively. The temperature was kept at 25°C, and the number of zeta runs was 26.8. As shown in the results, the zeta size of the impregnated nanocomposites was 1,127 d.nm and the polydispersity index (PDI) was 1.000, which indicated that the sample had a broad size distribution as the value of the polydispersive index fell between 0 and 1. A value close to 1 was considered an indicator of the broad nature of the sample size (Nolte et al., 2012). The intercept was 1.24. As shown in the results, peak 1 appeared at 268.2 d.nm, with a standard deviation of 29.34 d.nm. The size distribution by intensity is provided (Figure 4).

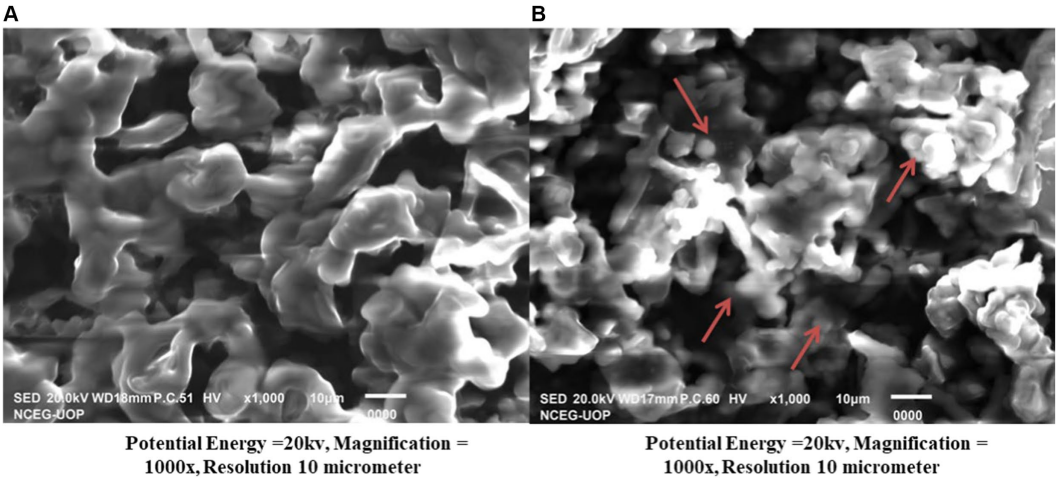

FIGURE 2
SEM analysis of **(A)** simple charcoal; **(B)** activated charcoal nanocomposites.

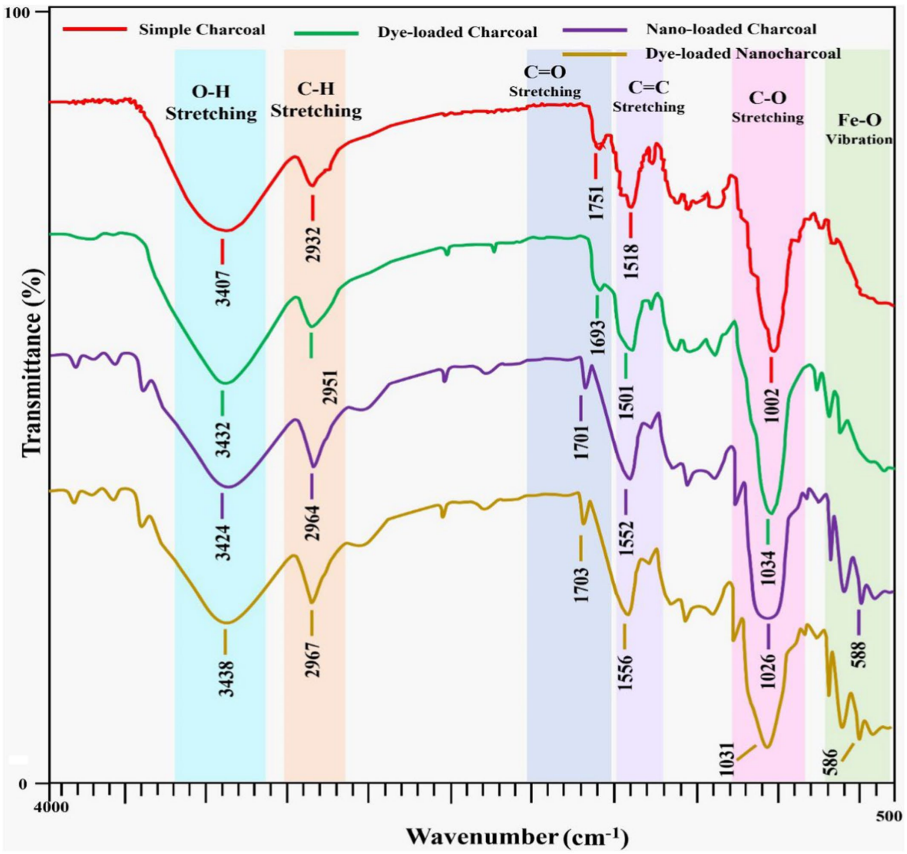

FIGURE 3
FTIR of simple charcoal (SC) and activated charcoal (Fe_2O_3/AC) nanocomposites (before and after adsorption).

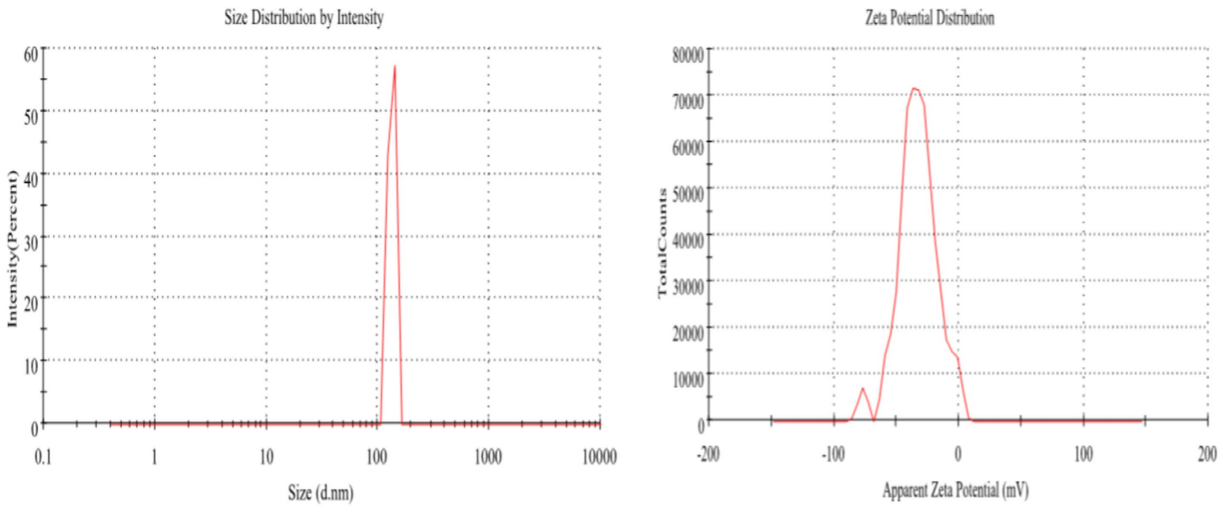

FIGURE 4
Particle size and zeta potential of composites.

The zeta potential was measured to be-32.9 mV in water, as shown in Figure 4. The zeta potential defined the stability behavior of the composites. CR is an anionic dye; these kinds of dyes have two azo groups on their surface in a solution form. Due to this, CR gives a negative value of zeta potential at pH 3 (Kant, 2012). As the zeta potential was found to be-32.9 mV, the zeta potential from ±30 to ±60 (mV) exhibited good stability of the composites, and it also showed that flocculation or agglomeration did not occur. Agglomeration only

occurs if the zeta potential values are low. The results were in good agreement with the reported data (Caon et al., 2010; Clogston and Patri, 2011; Mahajan and Ramana, 2014; Alsharef et al., 2017; Bhargava et al., 2018).

The BET analysis was performed on activated charcoal nanocomposites (before adsorption). The N_2 adsorption–desorption isotherm, as given in Figure 5, depicted a Type III isotherm. The surface area was found to be 2.562 m^2/g, and the total pore volume was 1.228e-03 cm^3/g for pores smaller than 2.6 nm (diameter) at P/Po = 0.30207. The pore volume, which was determined by the V-t method (micropore analysis), was found to be 0.008cm^3/g, the pore area was found to be 16.613m^2/g, and the external surface area was-14.051m^2/g.

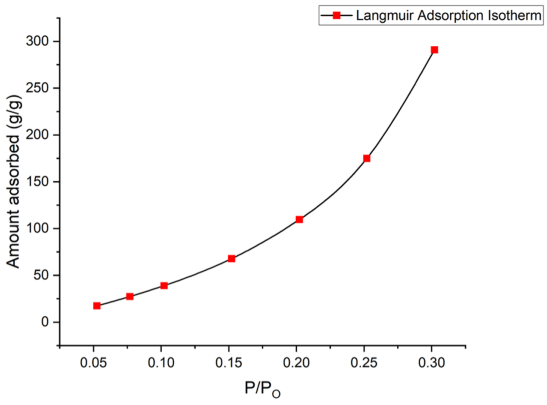

FIGURE 5
N_2 adsorption–desorption curve.

The effect of the heating rate was observed on the synthesized composites by conducting thermogravimetric analysis. Figure 6 depicts the changes observed in the weight of the composites by heating. Initially, the weight of the sample was 11.29 mg at 17°C, and the initial heating of the adsorbent showed a slight weight loss. Almost an 11% loss of weight was observed until 380°C. This initial weight loss can be attributed to moisture contents present in the adsorbent. A major weight loss of 62% was observed from 380°C to 450°C due to the decomposition of cellulose and lignin, as reported in previous studies on the decomposition of activated carbon (Niazi et al., 2018). The thermal stability of the synthesized composites provides good evidence for its use even at elevated temperatures. The differential thermal analysis (DTA) curve showed a positive heat flow toward the adsorbent from room temperature to 380°C, which played a role in the decomposition of some parts of the cellulose and moisture removal from the sample. Owing to cellulose decomposition being an endothermic reaction, during which heat is absorbed by composites, a difference in temperature between the sample and reference was created. To overcome this difference, a flow of heat occurred toward the sample pan to compensate for the change in heat; hence, a positive heat flow was observed. Then, the heat was released in the second part from 380°C to 650°C due to the decomposition of lignin, as shown in Figure 6.

Table 1 shows the weight loss observed at variable temperatures and weight percentages of the composites. After the thermal analysis, the remaining residual was 2.289 mg. This residual was subjected to FTIR for the determination of functional groups present to understand the residual composition.

Figure 7 shows the FTIR spectra of the thermal residue left after heating. The presence of prominent peaks in the ranges of 545 nm and 470 nm confirmed the presence of iron in the synthesized composites (Safa et al., 2011), as Metal was left behind after the decomposition of the organic components of the synthesized composites (Table 2).

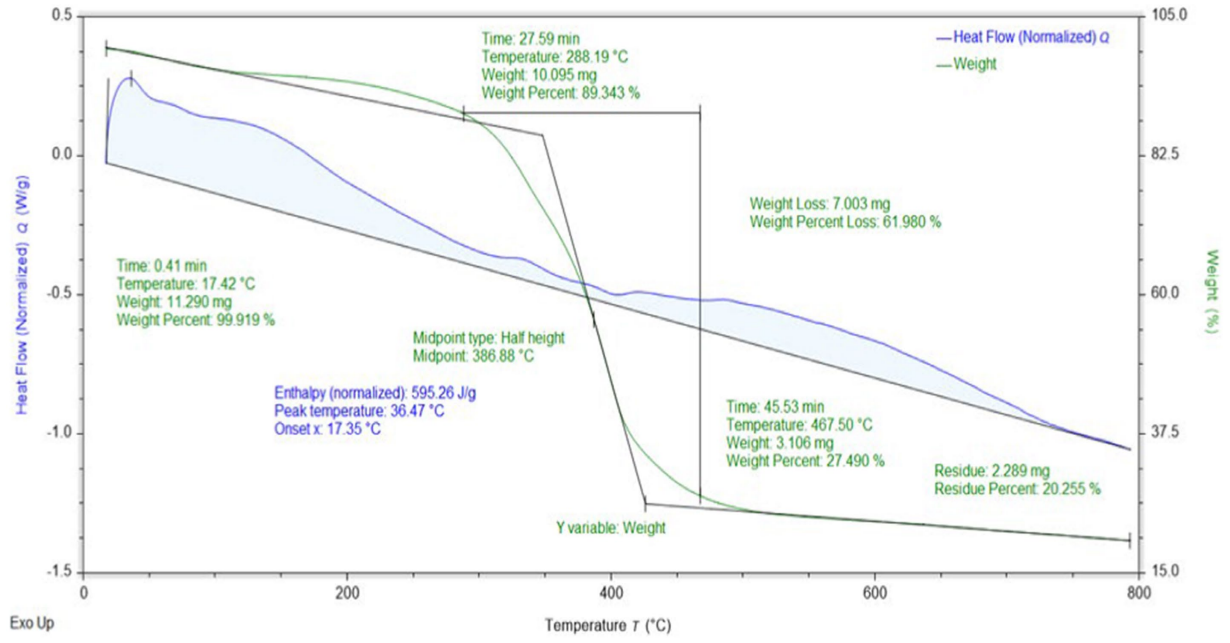

FIGURE 6
TGA and DTA results of synthesized composites.

3.2 Parameters optimization

Adsorption tests employing the batch adsorption method were carried out to determine the best conditions for removing the Congo red dye from aqueous solutions by altering several variables, such as pH value, contact time, initial adsorbate concentration, temperature, and amount of adsorbent (Figure 8).

After the experiment, the results showed that maximum absorbance was achieved at the concentration of 100 mg/L for both simple charcoal and activated charcoal nanocomposites. The adsorption capacity and adsorption rate were 8.577 mg/g and 85.75% for the simple charcoal, and an increased value of 9.21 mg/g adsorption capacity and 92.098% adsorption rate was observed for the activated charcoal nanocomposites. At low dye concentrations, the adsorption was also low as a smaller number of dye molecules were available for attachment on the surface of the sorbent. As dye concentrations increased, the adsorption also increased, and a maximum adsorption capacity was achieved at 100 mg/L (Table 3).

The data obtained revealed that the maximum adsorption capacity of 8.563 mg/g and 8.92 mg/g occurred at 30 min for both adsorbents, respectively. After that, the adsorption decreased because all active sites were already saturated with dye molecules and an increase in the contact time had no effect on the adsorption. Performing adsorption in a short time by a selected adsorbent is an advantage of the adsorbent. Maximum dye removal can be achieved in small time intervals (Table 4).

TABLE 1 Parameters and weight loss observed in TGA.

Time	Temperature	Weight	Weight percent
0.41 min	17.42°C	11.290 mg	99.919%
27.59 min	288.19°C	10.095 mg	89.343%
45.53 min	467.50°C	3.106 mg	27.490%
Residual Left		2.289 mg	

The results obtained showed that maximum adsorption occurs at 1 g/L if simple charcoal is used. The same reaction was repeated for the activated charcoal nanocomposites, with the fixed conditions of a 100 mg/L adsorbate concentration and 30 min of contact time. The results obtained showed that an adsorbent dosage of 0.75 g/L resulted in maximum adsorption in the case of the activated charcoal nanocomposites. Activated charcoal nanocomposites have better efficiency than simple charcoal and provide significant adsorption of dye with a small amount of adsorbent.

The effect of different temperature conditions on the adsorption potential was also observed. The results indicated that maximum absorbance will be at room temperature of 20°C for both simple charcoal and activated charcoal nanocomposites. Increasing the temperature by heating the solutions results in a decrease in absorbance. This decrease in the adsorption of a dye on heating may be an attachment of dye molecules due to the random movement of dyes at high-temperature conditions. As temperature increases, the entropy of the system also increases, which increases randomness.

Dye adsorption was analyzed under acidic, basic, and neutral conditions with a 100 ppm concentration of the dye with a 30 min contact time for 1 g activated carbon and a 100 ppm concentration of the dye with a 30 min contact time in an orbital shaker for 0.75 g activated charcoal nanocomposites. The results obtained showed that maximum adsorption occurred under acidic conditions as electrostatic attraction developed between the adsorbent and dye under the acidic mode of the reaction solution (Periyasamy and Viswanathan, 2019).

3.3 Adsorption isotherms

The isotherm equations were studied in the present research for the analysis of equilibrium data. At a constant temperature, the relationship between the adsorbed amount of a substance and its concentration in equilibrium is known as an adsorption isotherm.

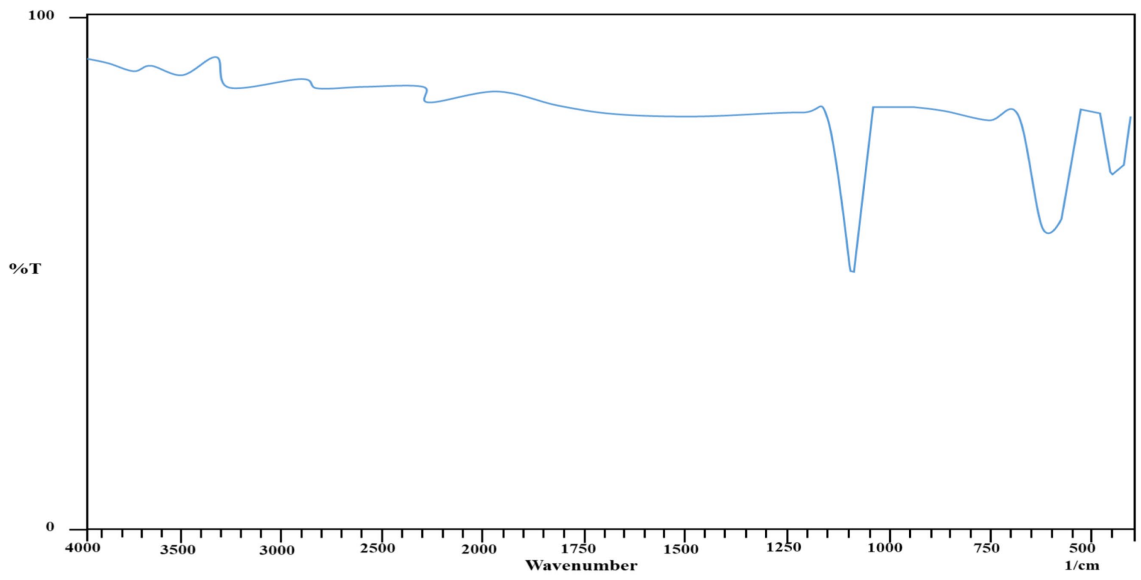

FIGURE 7
FTIR spectra of the residue left after TGA Analysis.

TABLE 2 Constant isotherms and parameters determined for the Congo red dye adsorption process.

Models		Adsorbent	
	Parameters	SC	Fe_2O_3/AC
Langmuir	q_m (mg/g)	0.8076	1.089
	K_L (L/mg)	0.117	0.114
	R_L	0.0787	0.081
	R^2	0.94077	0.95093
Freundlich	1/n	0.262	0.252
	K_F (mg/g (L/mg)$^{1/n}$)	0.0035	0.0022
	R^2	0.9816	0.9791
Dubinin–Radushkevich (D–R)	E (kJ/mol)	166.945	175.13
	q_{mDR} (mg/g)	34.318	31.9995
	K_{DR} (mol^2/J^2)	1.79305E-5	1.6311E-5
	R^2	0.97821	0.97456
Temkin	B_T (kJ/mol)	15.5009	16.05703
	K_T (L/g)	0.2008	0.204682
	R^2	0.8911	0.89242

From a theoretical and practical point of view, adsorption isotherms play an important role. For each system, an adsorption isotherm is important for establishing the correlation of the equilibrium data for the optimization of the design of the adsorption system for dye removal (Marandi and Sepehr, 2011). Sorption studies were carried out by implementing both linear and non-linear adsorption models. There are various isotherms equations known for solid–liquid systems. Freundlich isotherm, Langmuir isotherm, Dubinin–Radushkevich (D–R), and Temkin isotherm are applied in both a linear and non-linear form. For single solute systems, the most widely accepted surface adsorption models are Langmuir (2) and Freundlich isotherms (1) (Ho and McKay, 1999) (Figure 9) (Eqs 1, 2).

$$Inqe = \ln K_F + \frac{1}{n} InCe \left(\text{linear form}\right) \tag{1}$$

$$q_e = K_F C_e^{1/n} \left(\text{non} - \text{linear form}\right)$$

$$qe = \frac{q_m K_L C_e}{1 + K_L C_e} \tag{2}$$

where q_e (mg/g) is the adsorption capacity; C_e is the equilibrium dye concentration; q_m is the maximum capacity of dye adsorption; K_F (mg/g (mg/L)$^{1/n}$) and K_L (L/mg) are the constants of Freundlich and Langmuir isotherms, respectively, and n is the empirical constant showing adsorption intensity, which depends on the heterogeneity of the materials used as adsorbents and varies accordingly (Figure 10).

The Dubinin–Radushkevich model is also used, where ln q_e vs. potential energy (ε) is plotted at various temperatures to determine mean free energy, which aids in understanding the physical or chemical nature of adsorption processes. Polanyi potential (ε) can be calculated through (Eq. 3), and the mean free energy of adsorption is determined using (Eq. 4).

$$\ln q_e = \ln q_{mDR} - K_{DR}\mu^2$$

$$\mu = \mathrm{RT}\ln\left(1 + \frac{1}{C_e}\right) \tag{3}$$

$$E = \frac{1}{\sqrt{2K_{DR}}} \tag{4}$$

The Temkin model is also used to plot a graph between q_e and In C_e using the equation, where B_T (R_T/b) is the heat of adsorption (J/mol); R is the gas constant (8.314 J/mol K); T is the absolute temperature (K); and K_T = Temkin equilibrium constant (L/g) is attributed to the maximum binding energy (Figure 11).

$$qe = \frac{RT}{B_T}\ln K_T + \frac{RT}{B_T}\ln C_e$$

3.4 Adsorption kinetics

Details on ideal conditions, sorption mechanisms, and potential rate-limiting phases are included in kinetic studies for batch adsorption systems (Sahu et al., 2020). For this purpose, pseudo-first-order and pseudo-second-order linear kinetics were applied to the adsorption data, as shown in Eqs 5, 6, respectively.

A 1000 mg/L concentration solution of the Congo red dye was prepared, and 8 mg/L of this sample was used to look at how the contact time—between 30 and 150 min—affected the adsorption. This Congo red solution received 1 g of sorbent, and it was shaken at 135 rpm. Each solution was removed after a predetermined amount of time, and the leftover dye concentration in the residual filtrate was assessed using a UV–visible spectrophotometer:

$$y = q_t\left(1 - \exp\left(-K_1 x\right)\right) \tag{5}$$

$$\frac{t}{q_t} = \frac{1}{K_2 q_e^2} \times \frac{t}{Q} + \frac{t}{q_e}, \tag{6}$$

where q_t (mg/g) and q_e (mg/g) were the amount of dye adsorbed at time t and equilibrium, respectively; K_1 and K_2 (min^{-1} and g/mg) were the pseudo-first-order and pseudo-second-order constants, respectively (Figure 12).

3.5 Thermodynamic study

The investigation of thermodynamic parameters is also important in adsorption studies for determining the spontaneity of the

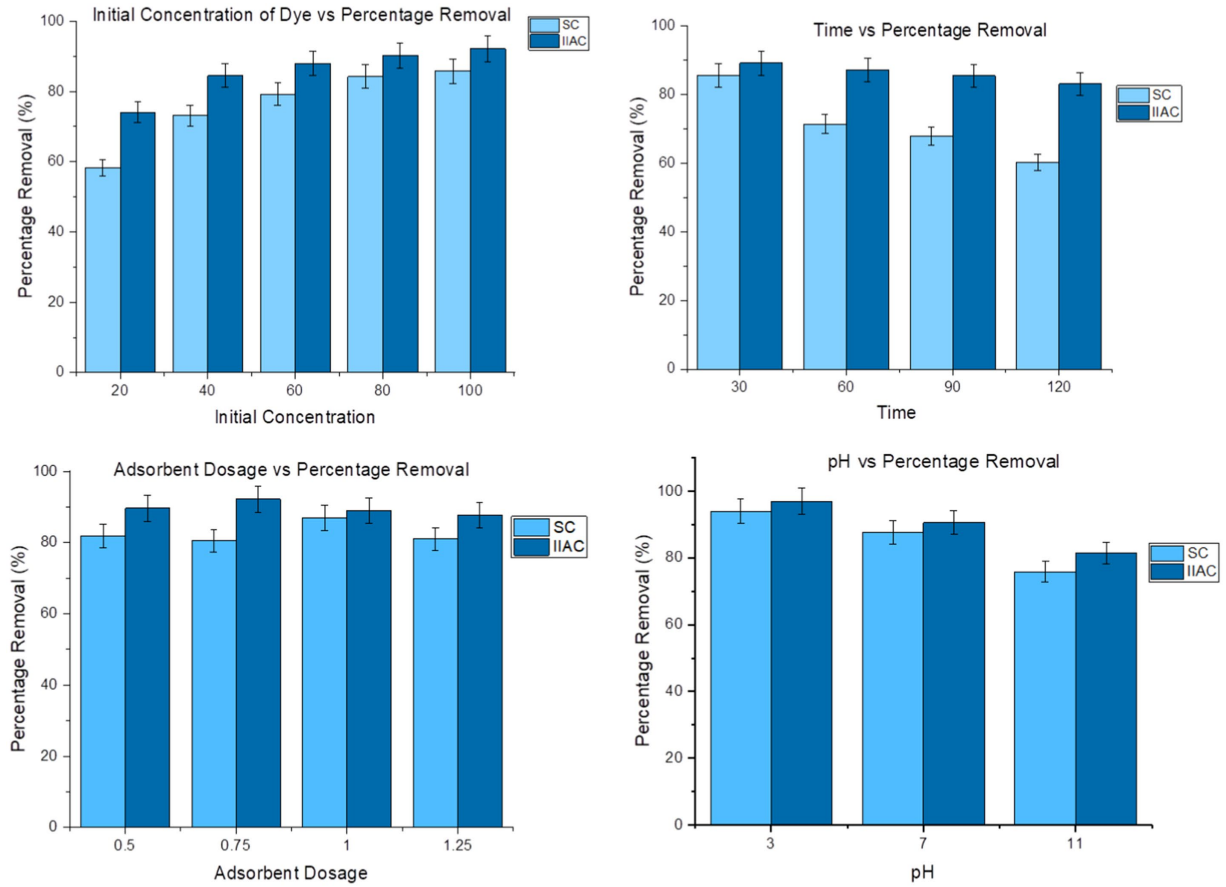

FIGURE 8
Effect of different adsorption parameters conditions (dye concentration, time, and pH value) on the adsorption of Congo red.

TABLE 3 Adsorption kinetic model parameters for the Congo red dye adsorption process.

Dyes	Pseudo-second-order				Pseudo-first-order		
	q_e	q_e^2	K_2	R^2	q_e	K_1	R^2
Congo red (with simple charcoal)	5.5503	30.806	−0.0144	0.99359	0.0103	0.0026475	0.6911
Congo red (with activated charcoal nanocomposites)	8.13273	66.1413	−0.0362	0.99943	0.212460328	0.0006205	0.97911

adsorption process, the adsorbent applicability, and the nature of the adsorption process. For conducting the investigation, the experiment was carried out at a different temperature, and then the calculation of different parameters, for example, Gibbs free energy (ΔG), enthalpy (ΔH), and entropy (ΔS) was done using the equation (Figure 13) (Eq 7).

$$\Delta G = \Delta H^{\circ} - T\Delta S^{\circ} \quad (7)$$

A graph was plotted between 1/T and ln K_L, where T was the temperature (kelvin) and K_L *(Langmuir constant)*, and ΔH and ΔS corresponded to slope and intercept, respectively.

In this step, five solutions of 100 ppm dye concentration were prepared, 1 g of simple charcoal was added to each solution, the temperature was maintained at 20, 30, 40, 50, and 60°C, respectively, and the solutions were shaken in an orbital shaker for 30 min. The results after

TABLE 4 Thermodynamic parameters for the Congo red dye adsorption process.

^0C	ΔG^0	ΔH^0	ΔS^0	R^2
20	0.99	−10.1796	−38.5520	0.93575
30	1.72			
40	1.84			
50	2.22			
60	2.66			
20	−0.35	−13.718	−45.702	0.95716
30	0.21			
40	0.42			
50	1.26			
60	1.40			

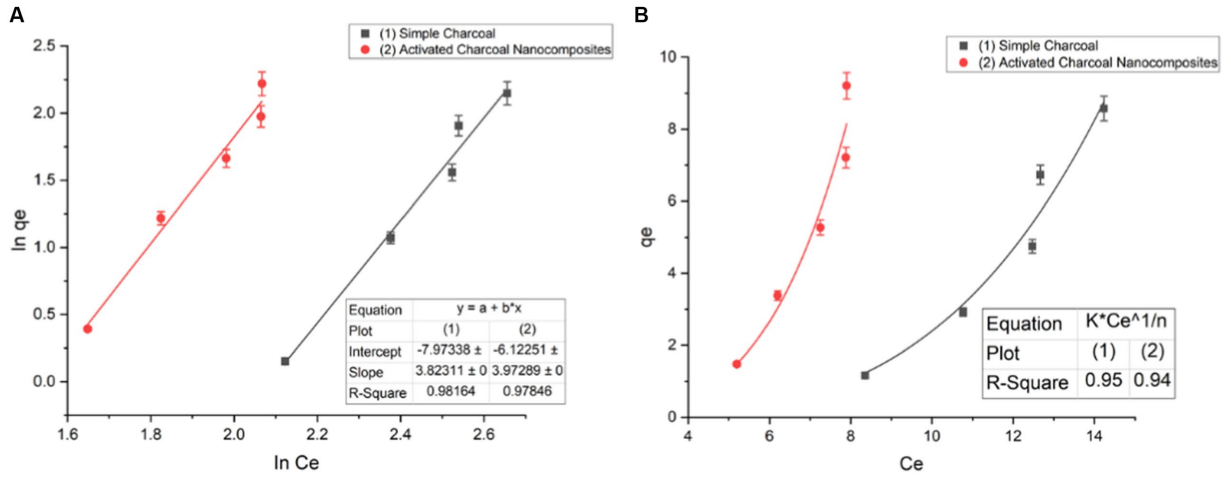

FIGURE 9
Freundlich isotherm of simple charcoal (SC) and activated charcoal (Fe_2O_3/AC) nanocomposite of a **(A)** linear form and **(B)** non-linear form (t = 120 min, pH = 7, dose = 1 g/L, and T = 20°C).

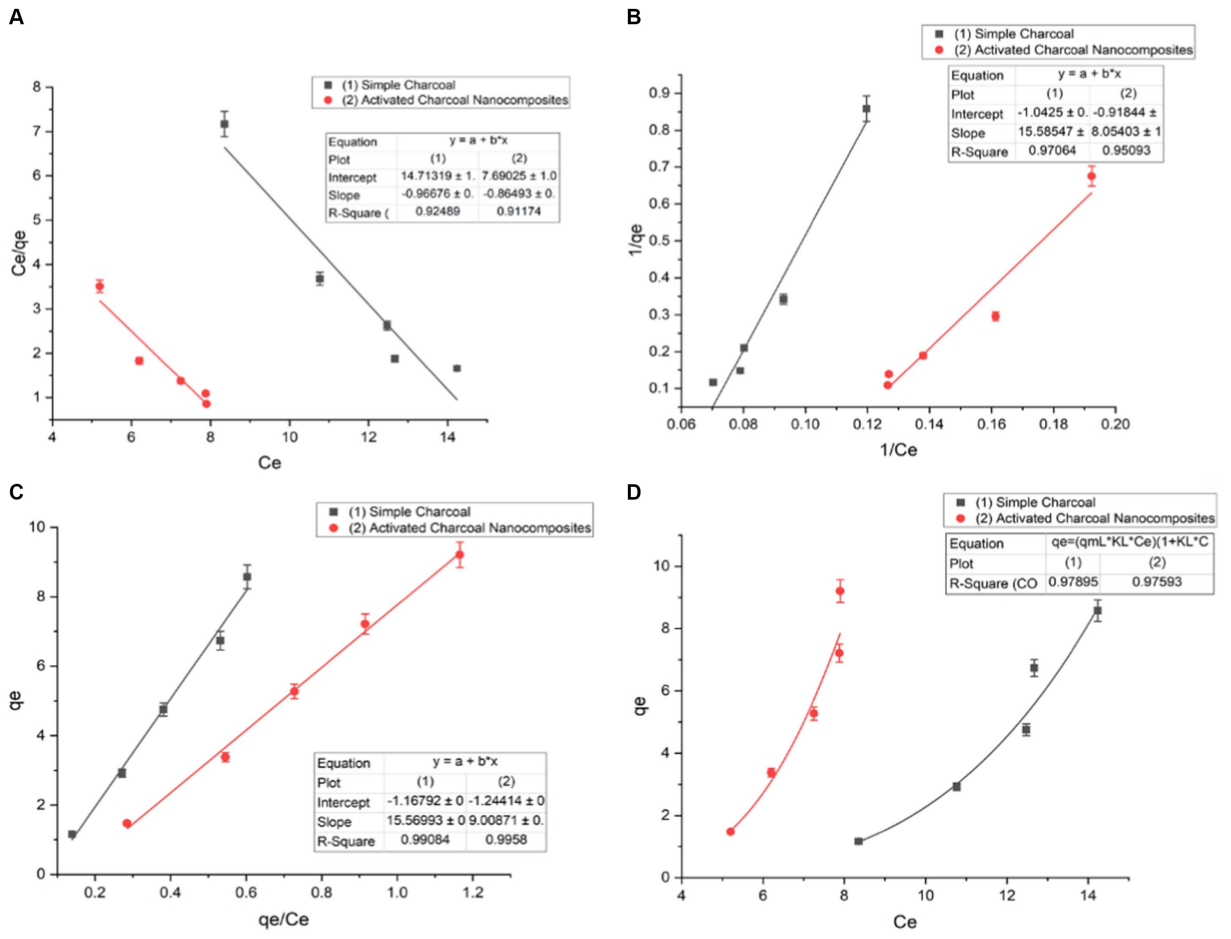

FIGURE 10
Langmuir isotherm of **(A)** type I linear form, **(B)** type II, **(C)** type III, and **(D)** non-linear form (t = 120 min, pH = 7, dose = 1 g/L, and T = 20°C).

the experiment showed that maximum absorbance would be at a room temperature of 20°C. Increasing the temperature by heating the solutions resulted in a decrease in absorbance. In the same way, five solutions of 100 ppm dye concentration were prepared, 0.75 g of activated charcoal nanocomposites were added to each solution, the temperature was maintained at 20, 30, 40, 50, and 60°C, respectively, and the solutions were shaken in an orbital shaker for 30 min. The results after the experiment were the same as for simple charcoal (Figure 14).

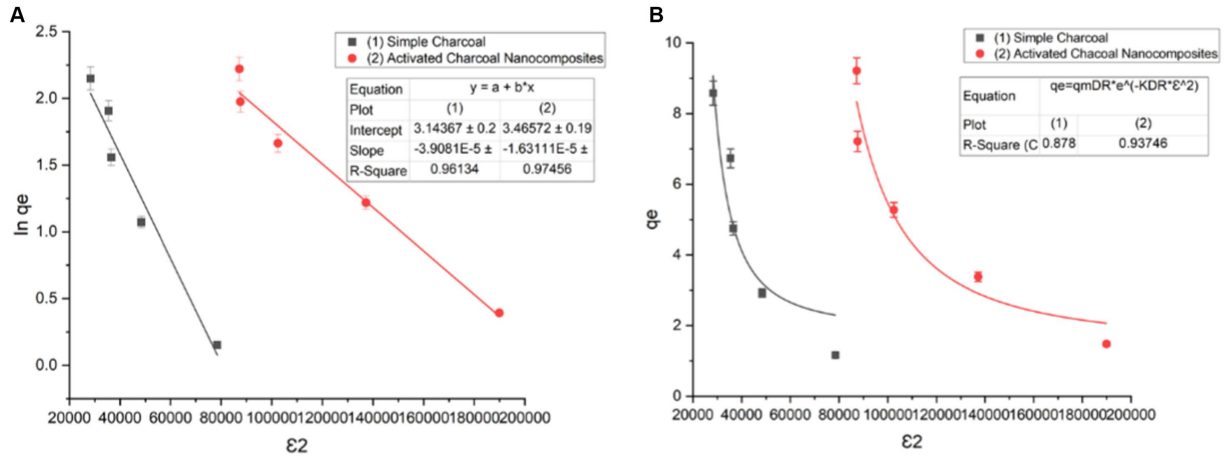

FIGURE 11
Dubinin–Radushkevich isotherm of **(A)** linear form and **(B)** non-linear form (t = 120 min, pH = 7, dose = 1 g/L, and T = 20°C).

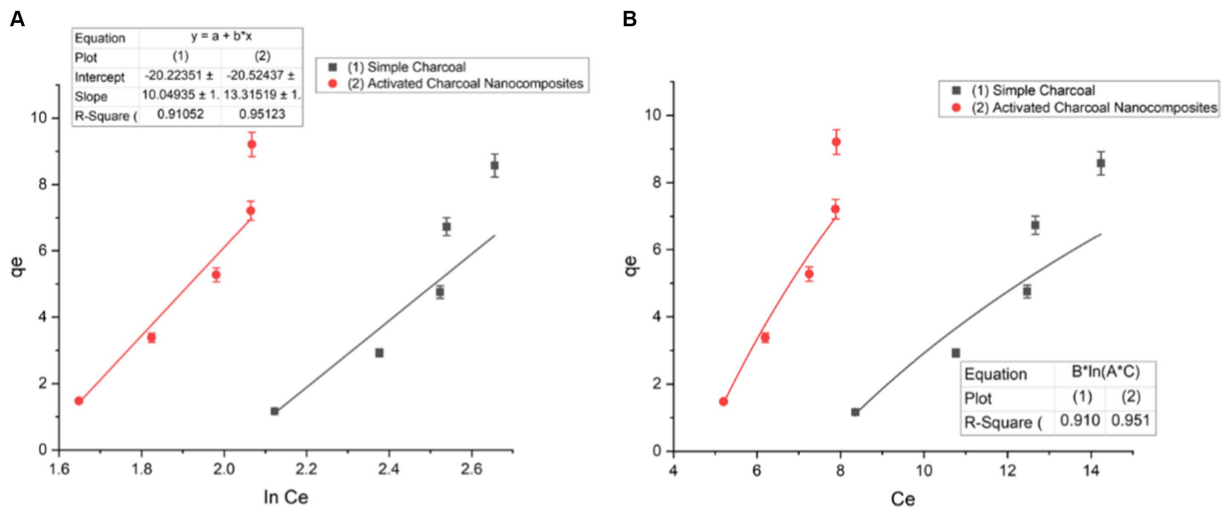

FIGURE 12
Temkin isotherm of **(A)** linear form and **(B)** non-linear form (t = 120 min, pH = 7, dose = 1 g/L, and T = 20°C).

According to the results, the value of ΔG for the Congo red dye adsorption process using SC and Fe_2O_3/AC magnetic nanocomposites had a negative value, which indicates that the adsorption process is spontaneous (Marandi and Sepehr, 2011). In addition, the value of the ΔH parameter for the Congo red dye adsorption process was determined using SC and Fe_2O_3/AC magnetic nanocomposites, −10.1796 kJ/mol and − 13.718 kJ/mol, respectively, which shows that the adsorption process is exothermic. Furthermore, the value of the ΔS parameter was negative, as determined by the adsorption process, proving that irregularities and random collisions at the adsorbent surface are reduced during the adsorption process. Based on the results, it can be concluded that the parameter ΔH has a greater effect than ΔS in determining the negative value of ΔG (Dehghani et al., 2021) (Figure 15).

3.6 Regeneration of adsorbent

Synthesized adsorbents can be regenerated if again applied for the removal of a dye in a cyclic process. This cyclic regeneration of adsorbents makes it more applicable for environmental remediation. Figure 16 shows the regeneration and reuse of adsorbents for the removal of Congo red dye from aqueous media.

Simple charcoal and **activated charcoal nanocomposites** were applied for the regeneration experiment by using ethanol. Adsorbents were washed with ethanol for 30 min, and the adsorbed dye was removed. Regenerated adsorbents were again applied for the same experiment. Although the efficiency of the adsorbent reduces at every cycle of regeneration due to the persistent attachment of some molecules with the adsorbent surface, significant removal is achieved (Bensalah et al., 2020).

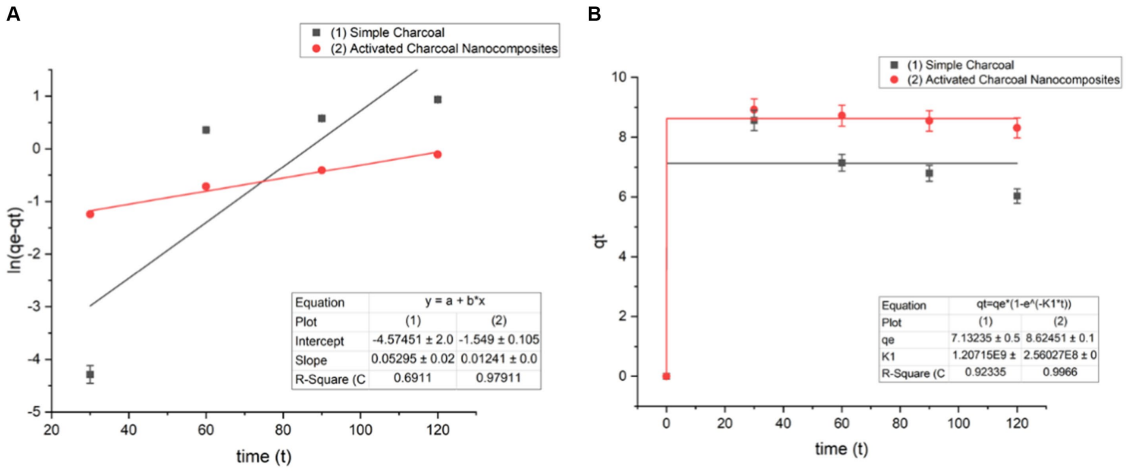

FIGURE 13
Pseudo-first-order kinetics of a **(A)** linear form and **(B)** non-linear form (C_o = 100 mg/L, pH = 7, dose = 1 g/L, and T = 20°C).

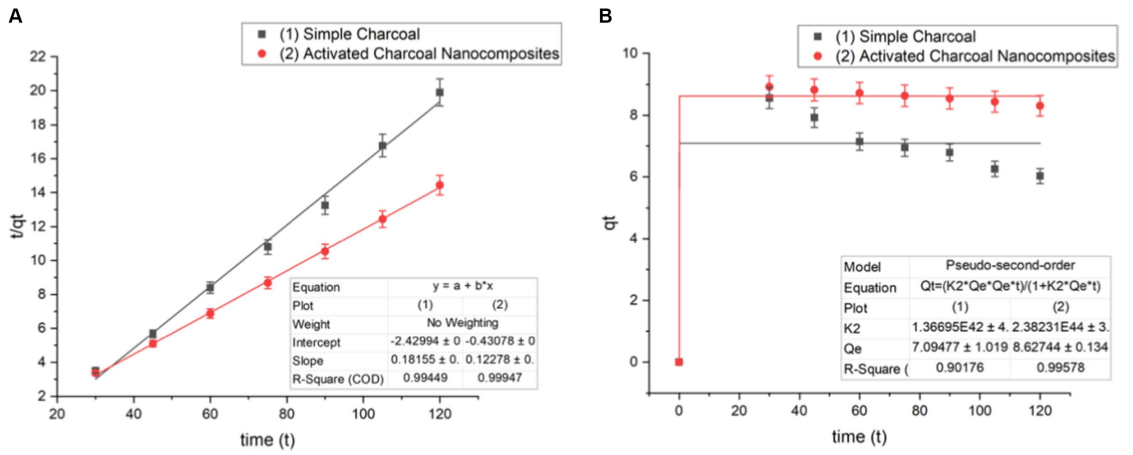

FIGURE 14
Pseudo-second-order kinetics of a **(A)** linear form and **(B)** non-linear form (C_o = 100 mg/L, pH = 7, dose = 1 g/L, and T = 20°C).

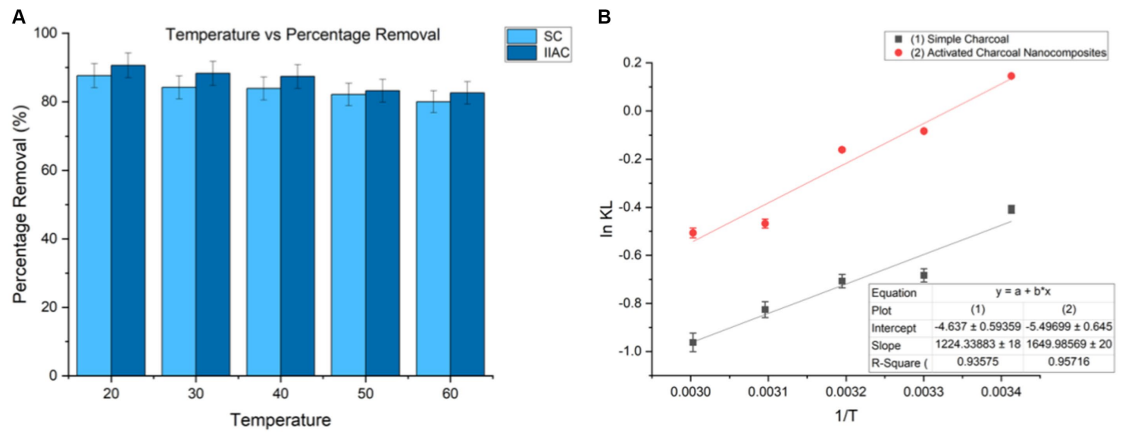

FIGURE 15
(A) Graph showing the effect of temperature on percentage removal and **(B)** Van't Hoff plot for the adsorption of Congo red Dye (C_o = 100 mg/L, pH = 7, dose = 1 g/L and 0.75 g/L, and *t* = 30 min).

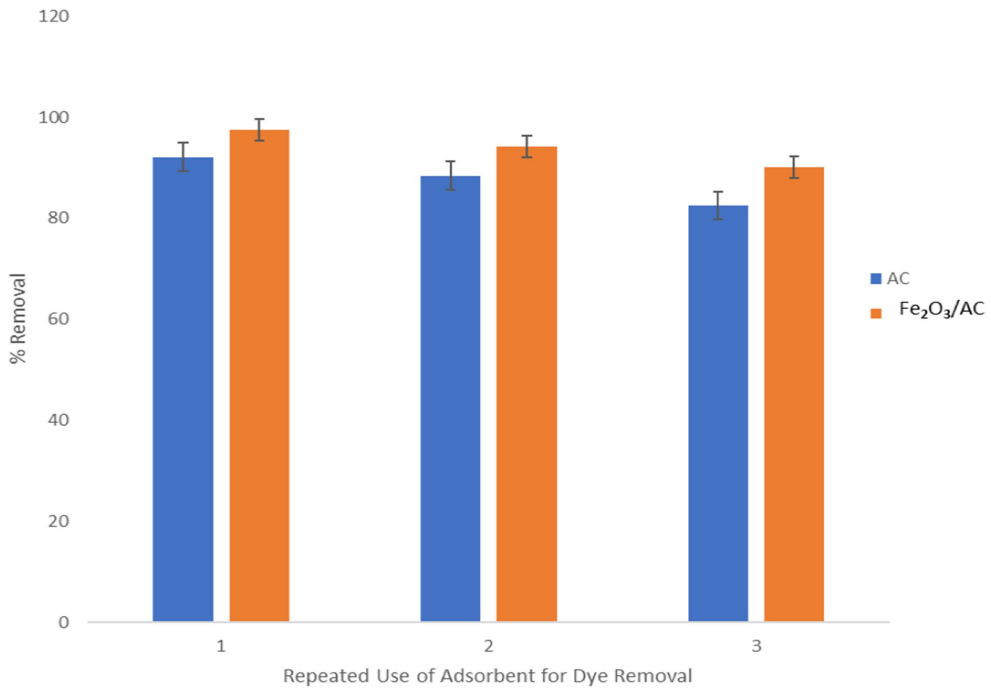

FIGURE 16
Regeneration and reuse of adsorbents for Congo red remediation (C_o = 100 mg/L, t = 30 min, pH = 3, dose = 1 g/L and 0.75 g/L, and T = 20°C).

4 Conclusion

The removal of Congo red dye from an aqueous solution was performed by using simple charcoal and activated charcoal nanocomposites of *C. sinensis*. The results obtained indicated that the efficiency of the adsorbent was exceptional and showed that selected adsorbents can be utilized for the elimination of Congo red dye from aqueous media to purify industrial wastewater. To determine the appropriate correlation for the elimination of dyes, four adsorption isotherms were used to analyze the experimental data, including Langmuir, Freundlich, Dubinin–Radushkevich, and Temkin isotherms. The linear form of Freundlich and Langmuir isotherms was the best fit for the experimental data, while Dubinin–Radushkevich helped determine the physical nature of the adsorption. The kinetic model was also applied to the experimental data; the highest linear regression coefficient (R^2) showed that the system was best explained by a pseudo-second-order kinetic model. In this adsorption study, it was also found that more adsorption of the Congo red dye occurred at a high initial concentration of the dye, a high concentration of the adsorbent, a small contact time, and under acidic conditions. This newly developed idea of using de-oiled seeds for the synthesis of simple charcoal and then iron oxide loading onto it makes it a suitable choice for environmental remediation, and it is a step toward the green and clean application of waste material for beneficial purposes.

Data availability statement

The raw data supporting the conclusions of this article will be made available by the authors, without undue reservation.

Author contributions

MT: Writing – original draft, Methodology. FB: Project administration, Writing – review & editing. SN: Writing – review & editing. MM: Software, Writing – review & editing. KM: Data curation, Writing – review & editing. SK: Software, Writing – review & editing. KS: Methodology, Writing – review & editing. AA: Writing – review & editing, Validation. HA: Funding acquisition, Writing – review & editing.

Funding

The author(s) declare financial support was received for the research, authorship, and/or publication of this article. This work was funded by the Researchers Supporting Project number (RSP2024R123), King Saud University, Riyadh, Saudi Arabia.

Acknowledgments

The authors would like to extend their sincere appreciation to the Researchers Supporting Project number (RSP2024R123), King Saud University, Riyadh, Saudi Arabia.

Conflict of interest

The authors declare that the research was conducted in the absence of any commercial or financial relationships that could be construed as a potential conflict of interest.

Publisher's note

References

Adebisi, G. A., Chowdhury, Z. Z., and Alaba, P. A. (2017). Equilibrium, kinetic, and thermodynamic studies of lead ion and zinc ion adsorption from aqueous solution onto activated carbon prepared from palm oil mill effluent. *J. Clean. Prod.* 148, 958–968. doi: 10.1016/j.jclepro.2017.02.047

Adegoke, K. A., and Bello, O. S. (2015). Dye sequestration using agricultural wastes as adsorbents. *Water Resour. Ind.* 12, 8–24. doi: 10.1016/j.wri.2015.09.002

Akbari, A., Remigy, J., and Aptel, P. (2002). Treatment of textile dye effluent using a polyamide-based nanofiltration membrane. *Chem. Eng. Process. Process Intensif.* 41, 601–609. doi: 10.1016/S0255-2701(01)00181-7

Al-Bastaki, N. (2004). Removal of methyl orange dye and Na2SO4 salt from synthetic waste water using reverse osmosis. *Chem. Eng. Process. Process Intensif.* 43, 1561–1567. doi: 10.1016/j.cep.2004.03.001

Alencar, W. S., Acayanka, E., Lima, E. C., Royer, B., de Souza, F. E., Lameira, J., et al. (2012). Application of Mangifera indica (mango) seeds as a biosorbent for removal of Victazol Orange 3R dye from aqueous solution and study of the biosorption mechanism. *Chem. Eng. J.* 209, 577–588. doi: 10.1016/j.cej.2012.08.053

Alsharef, J. M., Taha, M. R., and Khan, T. A. (2017). Physical dispersion of nanocarbons in composites—a review. *Jurnal Teknologi* 79, 69–81. doi: 10.11113/jt.v79.7646

Annadurai, G., Juang, R.-S., and Lee, D.-J. (2002). Use of cellulose-based wastes for adsorption of dyes from aqueous solutions. *J. Hazard. Mater.* 92, 263–274. doi: 10.1016/S0304-3894(02)00017-1

Arslan, I., Balcioğlu, I. A., and Bahnemann, D. W. (2000). Advanced chemical oxidation of reactive dyes in simulated dyehouse effluents by ferrioxalate-Fenton/UV-A and TiO2/UV-A processes. *Dyes Pigments* 47, 207–218. doi: 10.1016/S0143-7208(00)00082-6

Banat, I. M., Nigam, P., Singh, D., and Marchant, R. (1996). Microbial decolorization of textile-dyecontaining effluents: a review. *Bioresour. Technol.* 58, 217–227. doi: 10.1016/S0960-8524(96)00113-7

Banerjee, S., and Chattopadhyaya, M. (2017). Adsorption characteristics for the removal of a toxic dye, tartrazine from aqueous solutions by a low cost agricultural by-product. *Arab. J. Chem.* 10, S1629–S1638. doi: 10.1016/j.arabjc.2013.06.005

Bensalah, H., Younssi, S. A., Ouammou, M., Gurlo, A., and Bekheet, M. F. (2020). Azo dye adsorption on an industrial waste-transformed hydroxyapatite adsorbent: kinetics, isotherms, mechanism and regeneration studies. *J. Environ. Chem. Eng.* 8:103807. doi: 10.1016/j.jece.2020.103807

Bhargava, S., Chu, J. J. H., and Valiyaveettil, S. (2018). Controlled dye aggregation in sodium dodecylsulfate-stabilized poly (methylmethacrylate) nanoparticles as fluorescent imaging probes. *ACS Omega* 3, 7663–7672. doi: 10.1021/acsomega.8b00785

Cai, Y., Shen, Y., Xie, A., Li, S., and Wang, X. (2010). Green synthesis of soya bean sprouts-mediated superparamagnetic Fe2O3 nanoparticles. *J. Magn. Magn. Mater.* 322, 2938–2943. doi: 10.1016/j.jmmm.2010.05.009

Caon, T., Zanetti-Ramos, B. G., Lemos-Senna, E., Cloutet, E., Cramail, H., Borsali, R., et al. (2010). Evaluation of DNA damage and cytotoxicity of polyurethane-based nano- and microparticles as promising biomaterials for drug delivery systems. *J. Nanopart. Res.* 12, 1655–1665. doi: 10.1007/s11051-009-9828-2

Castro, C. S., Guerreiro, M. C., Gonçalves, M., Oliveira, L. C., and Anastácio, A. S. (2009). Activated carbon/iron oxide composites for the removal of atrazine from aqueous medium. *J. Hazard. Mater.* 164, 609–614. doi: 10.1016/j.jhazmat.2008.08.066

Chavan, R. (2011). "Environmentally friendly dyes" in *Handbook of textile and industrial dyeing*, ed. M. Clark. 515–561.

Choudhry, A., Sharma, A., Khan, T. A., and Chaudhry, S. A. (2021). Flax seeds based magnetic hybrid nanocomposite: an advance and sustainable material for water cleansing. *J. Water Process Eng.* 42:102150. doi: 10.1016/j.jwpe.2021.102150

Clogston, J. D., and Patri, A. K. (2011). "Zeta potential measurement" in *Characterization of nanoparticles intended for drug delivery*, ed. J. M. Walker. 63–70.

Dehghani, Z., Sedghi-Asl, M., Ghaedi, M., Sabzehmeidani, M. M., and Adhami, E. (2021). Ultrasound-assisted adsorption of paraquat herbicide from aqueous solution by graphene oxide/mesoporous silica. *J. Environ. Chem. Eng.* 9:105043. doi: 10.1016/j.jece.2021.105043

Gong, D., Sun, L., Li, X., Zhang, W., Zhang, D., and Cai, J. (2023). Micro/nanofabrication, assembly, and actuation based on microorganisms: recent advances and perspectives. *Small Struct.* 4:2200356. doi: 10.1002/sstr.202370026

Ho, Y., and McKay, G. (1999). Comparative sorption kinetic studies of dye and aromatic compounds onto fly ash. *J. Environ. Sci. Health A* 34, 1179–1204. doi: 10.1080/10934529909376889

Ilankoon, N. (2014). Use of iron oxide magnetic nanosorbents for Cr (VI) removal from aqueous solutions: a review. *J. Eng. Res. Appl.* 4, 55–63.

Kant, R. (2012). Textile dyeing industry an environmental hazard. *J. Nat. Sci.* 4, 22–26. doi: 10.4236/ns.2012.41004

Khanpit, V. V., Tajane, S. P., and Mandavgane, S. A. (2023). Technoeconomic and life cycle analysis of soluble dietary fiber concentrate production from waste orange peels. *Waste Manag.* 155, 29–39. doi: 10.1016/j.wasman.2022.10.036

Laskar, N., and Kumar, U.. SEM, FTIR and EDAX studies for the removal of safranin dye from water bodies using modified biomaterial-Bambusa tulda. In IOP Conference Series: Materials Science and Engineering. (2017). Beijing, China: IOP Publishing, 225, 012105.

Lin, S. H., and Lin, C. M. (1993). Treatment of textile waste effluents by ozonation and chemical coagulation. *Water Res.* 27, 1743–1748. doi: 10.1016/0043-1354(93)90112-U

Lompe, K. M., Menard, D., and Barbeau, B. (2017). The influence of iron oxide nanoparticles upon the adsorption of organic matter on magnetic powdered activated carbon. *Water Res.* 123, 30–39. doi: 10.1016/j.watres.2017.06.045

Lompe, K. M., Vo Duy, S., Peldszus, S., Sauvé, S., and Barbeau, B. (2018). Removal of micropollutants by fresh and colonized magnetic powdered activated carbon. *J. Hazard. Mater.* 360, 349–355. doi: 10.1016/j.jhazmat.2018.07.072

Mahajan, A., and Ramana, E. V. (2014). *Patents on magnetoelectric multiferroics and their processing by electrophoretic deposition.* Recent patents on. *Mater. Sci.* 7, 109–130. doi: 10.2174/1874464807666140701190424

Marandi, R., and Sepehr, S. M. B. (2011). Removal of Orange 7 dye from wastewater used by natural adsorbent of Moringa oleifera seeds. *Am. J. Environ. Eng.* 1, 1–9. doi: 10.5923/j.ajee.20110101.01

Martin, R. W. Jr., Baillod, C. R., and Mihelcic, J. R. (2005). Low-temperature inhibition of the activated sludge process by an industrial discharge containing the azo dye acid black 1. *Water Res.* 39, 17–28. doi: 10.1016/j.watres.2004.07.031

Meyer, V., Carlsson, F., and Oellermann, R. (1992). Decolourization of textile effluent using a low cost natural adsorbent material. *Water Sci. Technol.* 26, 1205–1211. doi: 10.2166/wst.1992.0562

Nassar, M. M., and El-Geundi, M. S. (1991). Comparative cost of colour removal from textile effluents using natural adsorbents. *J. Chem. Technol. Biotechnol.* 50, 257–264. doi: 10.1002/jctb.280500210

Niazi, L., Lashanizadegan, A., and Sharififard, H. (2018). Chestnut oak shells activated carbon: preparation, characterization and application for Cr (VI) removal from dilute aqueous solutions. *J. Clean. Prod.* 185, 554–561. doi: 10.1016/j.jclepro.2018.03.026

Nolte, H., Schilde, C., and Kwade, A. (2012). Determination of particle size distributions and the degree of dispersion in nanocomposites. *Compos. Sci. Technol.* 72, 948–958. doi: 10.1016/j.compscitech.2012.03.010

Parvin, S., Biswas, B. K., Rahman, M. A., Rahman, M. H., Anik, M. S., and Uddin, M. R. (2019). Study on adsorption of Congo red onto chemically modified egg shell membrane. *Chemosphere* 236:124326. doi: 10.1016/j.chemosphere.2019.07.057

Periyasamy, S., and Viswanathan, N. (2019). Hydrothermal synthesis of melamine-functionalized covalent organic polymer-blended alginate beads for iron removal from water. *J. Chem. Eng. Data* 64, 2280–2291. doi: 10.1021/acs.jced.8b01085

Pour, Z. S., and Ghaemy, M. (2015). Removal of dyes and heavy metal ions from water by magnetic hydrogel beads based on poly (vinyl alcohol)/carboxymethyl starch-g-poly (vinyl imidazole). *RSC Adv.* 5, 64106–64118. doi: 10.1039/C5RA08025H

Raghu, S., and Basha, C. A. (2007). Chemical or electrochemical techniques, followed by ion exchange, for recycle of textile dye wastewater. *J. Hazard. Mater.* 149, 324–330. doi: 10.1016/j.jhazmat.2007.03.087

Rathi, G., Siddiqui, S. I., and Pham, Q. (2020). Nigella sativa seeds based antibacterial composites: a sustainable technology for water cleansing-a review. *Sustain. Chem. Pharm.* 18:100332. doi: 10.1016/j.scp.2020.100332

Razi, M. A. M., Hishammudin, M. N. A. M., and Hamdan, R. "Factor affecting textile dye removal using adsorbent from activated carbon: a review," in MATEC Web of Conferences. Malaysia: EDP Sciences. (2017). 103:6015.

Rushing, L. G., and Bowman, M. C. (1980). Determination of gentian violet in animal feed, human urine, and wastewater by high pressure liquid chromatography. *J. Chromatogr. Sci.* 18, 224–232. doi: 10.1093/chromsci/18.5.224

Safa, Y., Bhatti, H. N., Bhatti, I. A., and Asgher, M. (2011). Removal of direct Red-31 and direct Orange-26 by low-cost rice husk: influence of immobilisation and pretreatments. *Can. J. Chem. Eng.* 89, 1554–1565. doi: 10.1002/cjce.20473

Sahoo, J. K., Hota, A., Khuntia, A. K., Sahu, S., Sahoo, S. K., Sabar, A. K., et al. (2022). Removal of dyes using various organic peel-based materials: a systematic review. *Appl. NanoBioSci.* 11, 3714–3727. doi: 10.33263/LIANBS113.37143727

Sahraei, R., Pour, Z. S., and Ghaemy, M. (2017). Novel magnetic bio-sorbent hydrogel beads based on modified gum tragacanth/graphene oxide: removal of heavy metals and dyes from water. *J. Clean. Prod.* 142, 2973–2984. doi: 10.1016/j.jclepro.2016.10.170

Sahu, S., Pahi, S., Tripathy, S., Singh, S. K., Behera, A., Sahu, U. K., et al. (2020). Adsorption of methylene blue on chemically modified lychee seed biochar: dynamic, equilibrium, and thermodynamic study. *J. Mol. Liq.* 315:113743. doi: 10.1016/j.molliq.2020.113743

Sarala, P., and Venkatesha, T. (2006). Electrochemical degradation of p-aminobenzoic acid β-naphthol azo dye in alkaline solution. *A-A* 10:100.

Sarioglu, M., and Atay, U. (2006). Removal of methylene blue by using biosolid. *Global NEST J.* 8, 113–120.

Shi, B., Li, G., Wang, D., Feng, C., and Tang, H. (2007). Removal of direct dyes by coagulation: the performance of preformed polymeric aluminum species. *J. Hazard. Mater.* 143, 567–574. doi: 10.1016/j.jhazmat.2006.09.076

Smith, B. (1986). Identification and reduction of pollution sources in textile wet processing. North Carolina State, US: Citeseer.

Smith, B. (1988). A workbook for pollution prevention by source reduction in textile wet processing United State: School of Textiles, North Carolina State University.

Song, W., Gao, B., Xu, X., Xing, L., Han, S., Duan, P., et al. (2016). Adsorption–desorption behavior of magnetic amine/Fe2O3 functionalized biopolymer resin towards anionic dyes from wastewater. *Bioresour. Technol.* 210, 123–130. doi: 10.1016/j.biortech.2016.01.078

Su, G., Chan, C., and He, J. (2022). Enhanced biobutanol production from starch waste via orange peel doping. *Renew. Energy* 193, 576–583. doi: 10.1016/j.renene.2022.04.096

Tan, K. A., Morad, N., Teng, T. T., Norli, I., and Panneerselvam, P. (2012). Removal of cationic dye by magnetic nanoparticle (Fe2O3) impregnated onto activated maize cob powder and kinetic study of dye waste adsorption. *APCBEE Procedia* 1, 83–89. doi: 10.1016/j.apcbee.2012.03.015

Tiadi, N., Mohanty, M., Mohanty, C. R., and Panda, H. P. (2017). Studies on adsorption behavior of an industrial waste for removal of chromium from aqueous solution. *S. Afr. J. Chem. Eng.* 23, 132–138.

Wang, C., Yediler, A., Lienert, D., Wang, Z., and Kettrup, A. (2003). Ozonation of an azo dye CI Remazol black 5 and toxicological assessment of its oxidation products. *Chemosphere* 52, 1225–1232. doi: 10.1016/S0045-6535(03)00331-X

Yao, S., Sun, S., Wang, S., and Shi, Z., Adsorptive removal of lead ion from aqueous solution by activated carbon/iron oxide magnetic composite. (2016).

Yuvaraja, G., Zheng, N. C., Pang, Y., Su, M., Chen, D. Y., Kong, L. J., et al. (2020). Removal of U (VI) from aqueous and polluted water solutions using magnetic Arachis hypogaea leaves powder impregnated into chitosan macromolecule. *Int. J. Biol. Macromol.* 148, 887–897. doi: 10.1016/j.ijbiomac.2020.01.042